Preprint Title	New styryl based organic chromophores including free amino and azomethine groups: Syntheses, photophysical, NLO and thermal properties
Authors	Anka U. Putra, Deniz Çakmaz, Nurgül Seferoğlu, Alberto Barsella and Zeynel Seferoğlu
Publication Date	23 Mär 2020
Article Type	Full Research Paper
Supporting Information File 1	SI.docx; 17.2 MB
ORCID® iDs	Zeynel Seferoğlu - https://orcid.org/0000-0002-1028-7231

New styryl based organic chromophores including free amino and azomethine groups: Syntheses, photophysical, NLO and thermal properties

Anka Utama Putra[1], Deniz Çakmaz[1], Nurgül Seferoğlu[2], Alberto Barsella[3], Zeynel Seferoğlu[1*].

Addresses:

[1]Gazi University, Department of Chemistry, 06500 Ankara, Turkey.

[2]Gazi University, Advanced Technology Department, 06500 Ankara, Turkey.

[3]De'partement d'Optique Ultra-Rapide et Nanophotonique, IPCMS, UMR CNRS, 7504, Universite' de Strasbourg, 23 Rue du Loess, BP 43, 67034 Strasbourg Cedex 2, France.

Email: Zeynel Seferoğlu – znseferoglu@gazi.edu.tr

* Corresponding author

Abstract

In this manuscript, we have successfully synthesized and characterized a new series of styryl based push-pull dyes containing free amino group and their Schiff bases derivatives in which dicyanomethylene was used as the acceptor group and different para-substituted alkylamines as the donor groups and 2-pyridyl as proton sensitive group. All compounds showed absorption in the visible region and green-red emission with low quantum yields. The photophysical properties were examined in various solvents with different polarities. The absorption and emission maxima were shifted

bathocromically by increasing solvents polarity however, there was no regular correlation with polarity parameter. Significant red shifts were observed in the absorption and fluorescence emission maxima on increasing the electron-donating ability of the substituents. The observed color changes were photographed naked eyes and under illuminating UV-lamp. The pH sensitive properties of newly prepared Schiff bases against TBAOH were examined inside DMSO, furthermore their reserve protonation were also investigated using TFA. The structural and electronic properties of all newly synthesized compounds were studied using DFT calculation. In addition, NLO property of compounds were investigated by DFT. For determination thermal properties of all compounds were investigated and they showed good thermal stability up to 250 $^{\circ}$C by TGA analyses under inert atmosphere. Our results indicate that the styryl based new push-pull dyes are promising candidate materials for NLO and pH applications.

Keywords

Styryl dyes; Schiff base; Solvent effect; pH sensitive dyes; NLO; DFT

Introduction

Push-pull organic molecules are a class of organic compound comprising of electron donating group in one end and electron withdrawing group in other end. This compound exhibits strong photophysical modulation when exposed to a passing wave of photons. This phenomenon caused by the structural modification that is triggered by significant electron migration and inevitable change in electronic composition during excited states. This change is followed by solvatochromic behavior, strong color

modulation and/or fluorescence increase. The changes observed generally explain how the molecule behave in a solution for its ground and excited state [1,2,3]. The important feature of this molecule class is exceptional polarizability which is crucial criterion for NLO materials. Nowadays extended π conjugation containing NLO materials have shown extensive usages particularly in signal processing, optical storage and telecommunication devices [4,5,6,7]. On the structural basis NLO chromophores are classified in two major groups: Inorganic and Organic based NLO chromophore [8,9]. Inorganic based NLO chromophores have to be isolated in single crystal form before their implementation that is not efficient and rewarding for commercial purposes nowadays. Fortunately the latter class NLO chromophores does not require such a thing to be implemented in advance, along with the flexibility to derivate their structures make them affordable candidates for implementation in various NLO devices [10]. The flexibility to swap electron donors and acceptors groups within the molecules gives us an ability to fine tune intramolecular charge transfer (ICT) intensity that comprehends chromophores NLO behaviors [11]. To understand the concept of NLO, first we may need to discuss about the first hyperpolarizability (β) value of a chromophore. Hyperpolarizability value indicates how convenient electron transfers occur within a molecule between the two ends, in this case electron donor and acceptor groups. Good NLO chromophores have usually a high value of both first and second hyperpolarizability, which explains intrinsically why push-pull molecules are good NLO chromophores. In order to inflate the total hyperpolarizability (β_{top}) value there is a necessity to pump electron density in the conjugation that is done by interchanging or adding stronger of either electron donor or acceptor groups. Furthermore, the electron density found within heterocycles in the push-pull system has a contribution in affecting β_{top} value of the system.

Hydroxide plays significance influences in environmental chemistry. Its presence in aqueous medium directly determining pH level that affects organisms living in the corresponding area [12]. For that, pH sensitive compounds are critical in various sensor applications. These compounds have a tendency to show different spectral properties upon protonation/deprotonation process [13].

Fluorescent dyes chemosensors posses unique merits such as low energy consumption, ease of handling and remarkable selectivity and notable sensitivity [14]. These traits makes them outstanding detecting capability in wide range of condition. Up until now, there are many investigations regarding pH sensitive fluorescent dyes with different approaches that led to an better understanding of hydroxide detection in organic or aquaeous environment however some failed to offer cheaper option due to synthesis complexities and/or expensive initial reagents. In the other hand, ICT in some fluorescent dyes is a notable characteristic that if optimized enough will trigger the appearence of NLO behavior. Among dyestuffs classes push-pull fluorescent dyes are renowned to own such special behaviors. These push pull dyes generate more charge delocalization upon excitation thus enhance both polarizability and fluorescence emission [15]. The charge delocalization upon excitation leads to redshifted emmision which is viable for various substrate detection in biological tissues and samples [16]. To address the aformentioned economical issues we introduced Schiff base which is easy and cheap to synthesis and pronounced for their for their antimicrobial, antifungal, antiviral and anticancer activity to the main structure of molecules investigated in the study [17,18]. Recently, there were massively growing interests in study regarding push pull organic molecules that makes use of dicyanomethylene group act as strong electron withdrawing group coupled with various donor conjugate through connecting π conjugation bridge [19,20,21,22]. Here, heterocyclic amines would be a great electron donating group thanks to their high electron density around nitrogen atom

[23,24]. Apart from that, heterocyclic amines have also makes their presences in various field from pharmaceutical to engineering and chemical sensing department [25,26,27,28,29,30,31,32]. Furthermore, a study regarding fluorescent probes [33] and NLO application for this compound has also been reported [34,35]. We have also conducted an NLO study for new series of styril based push-pull compounds in the last five years. Styryl compound contains unsaturated double bond, a structure similar to azomethine group, that connect electron donating and withdrawing group at its two ends. Based from the result alone, these compounds offers good NLO characteristic when compared to Disperse Red 1 as well as noteworthy thermal stability with dissociation temperatures for up to 300 ^{o}C [19,21].

Many have conducted study of plausible deprotonation process of bonded hydroxile group nearby ortho positioned azomethine bridge. While these approach can target certain anions however they show strong affinity towards cyanide and fluoride [20,36,37,38,39,40].

The azomethine bridge inside Schiff base is weak electron donating group. However, it still contributes to the total ICT thus increases molecular polarizability. This coupled with extended π conjugation will definitely makes a promising candidate for various NLO studies and applications [19,41,42,43].

Here, we report on syntheses and full photophysical characterization of a new series of styryl based organic compounds containing free amino group and their Schiff bases derivatives. The both series have various electron donating groups in the order of donor strength julolidine, pyrolidine, piperidine and morpholine. And also, it was synthesized additional two compounds bearing low pH sensitive 2-pyridinyl group. The pH sensitive properties of newly prepared Schiff bases against TBAOH were examined inside DMSO, furthermore their reverse protonation were also investigated using TFA. The obtained all photophysical changes were saved under UV-lamp and ambient light.

The structural and electronic properties of all newly synthesized compounds were studied using DFT calculation. To determine thermal properties for all compounds TGA analyses were done under inert atmosphere.

Results and Discussion

Synthesis

As depicted from Scheme 1 the reaction pathway starts from compound 1 (*2-(1-(4-aminophenyl)ethylidene)malononitrile*), its reaction with some benzaldehydes in mildly basic environment through aldol condensation gives compound **3-7** in moderate to good yields, generally without the need for chromatographic purification. Further reaction of compound **3-7** with salicylaldehyde in basic condition results a formation of azomethine bridge on each amine ends which gives compound **8-12** as final products. General procedures regarding the synthesis of both compounds are presented in the Scheme 1. The structures of the all new synthesized compounds were confirmed by FT-IR, ^{1}H/^{13}C NMR and HRMS (see SI). In addition, the stereochemistries of the double bonds in compounds were determined on the basis of the coupling constants of the vinylic hydrogens in the ^{1}H NMR spectra ($J \approx$ 15-16 Hz). The results show that the compounds are stable as *E* stereomer.
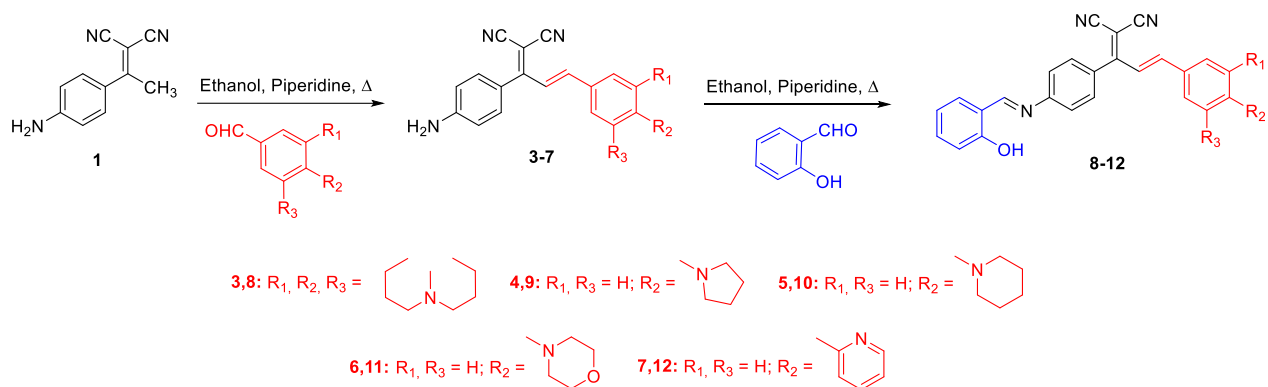
Scheme 1. General synthetic pathway of compounds **3-7** and **8-12**.

Optimized Geometries

The optimized geometries of compounds **3-7** and **8-12** were obtained by performing DFT calculations at B3LYP/631+g(d,p) level. The structures were demonstrated in Figure 1 and Figure S1 for **3-7** and **8-12**, respectively (see SI). It is obtained that variable substituents (-R_2, in Scheme 1) were planar with dicyanomethylene group. Relevant C4-C2-C1-C11 dihedral angles were about 179º for all compounds. An amount of twisting was observed between the dicyanomethylene and 4-aminophenyl group with angles of 49.6º, 48.4º, 48.3º, 47.7º, 46.8º and for **3-7**, respectively.

For **8-12**, dihedral angle of C46-C45-N40-C37 between phenyl and hydroxyphenyl groups was obtained about 177º; the twisting angle between dicyanomethylene and phenyl attached to the azomethine (C=N) bridge was about 50º; the dihedral angle C4-C2-C1-C11 was about 179º. However, as noticed from the Figure S1, compounds **8-12** exhibit O56-H57…N40 intramolecular strong hydrogen bond that has lengths of 2.636 Å, 2.634 Å, 2.633 Å, 2.635 Å, and 2.634 Å, respectively.
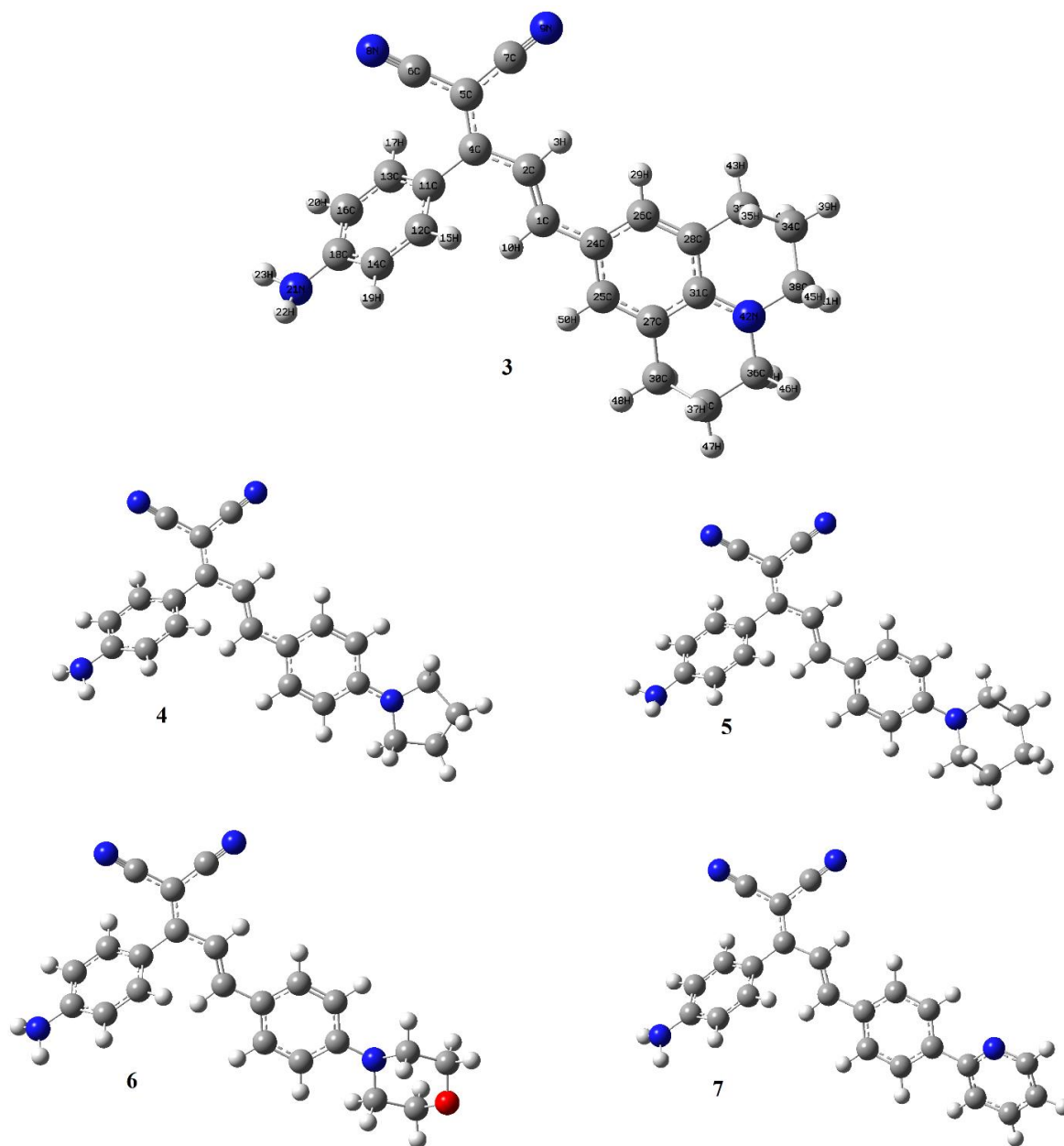
Figure 1. The optimized geometries of **3**-**7**.

Absorption and emission properties

To assess the effect of the solvent on the absorption and emission spectra of **3**-**7** and **8**-**12** (c=10 µM for absorption, and 1 µM for emission), various solvents with different polarity were employed at room temperature (Figure 2, Table 1 and Table S1, see

Photophysical Properties of Compounds **3-12** in SI). Unfortunately, many solvents mainly less-polar or non-polar could not be used because of the limited solubility of the analyte. The compounds have generally good solubility in organic solvents used in study however, the compounds **8-12** have enough solubility for determination in MeOH. For polarity Dimroth–Reichardt polarity parameters were used (E_T^{30}, Dimroth–Reichardt polarity parameter in kcal mol^{-1}, MeOH, 55.4, ACN, 45.6, DMSO, 45.1, DCM, 40.7, THF, 37.4, PhMe, 33.9). In addition, the absorption spectra of all compounds were obtained with TD-DFT calculations using the PCM model. The relevant data are given in Table 1 and Table S1 (see SI).

The shifts of the absorption maxima of these compounds are little dependent from the solvent polarity and there are small differences of absorption maxima values for both series. As representative examples, the spectra of compounds **3** and **8** are provided in Figure 2. The absorption spectra of **3** and **8** in all studied solvents displayed absorption maxima in the range of 512-543 and 529-562 nm, respectively. It is noted that the the largest bathochromic shifts of absorption maxima for both serie of compounds were observed in DMSO. From DMSO to toluene, the bathochromic shift was observed at 31 nm for **3**, at 22 nm for **4**, at 19 nm for **5** and at 23 nm for **6**. The similar behaviors were obtained for absorption spectra **8-12** (Table S1, see SI). In the calculations, it was obtained that the absorption wavelengths for the studied compounds changed in order **3**>**4**>**5**>**6**>**7** and also **8**>**9**>**10**>**11**>**12** in DMSO, as consistent with experimental data. The solvent effects on the absorption spectra were seen for **4** and **5** with a bathochromic shift about 16-17 nm from DMSO to toluene while the shifted was only 7 nm for **3** and **6**. In case of **8-11**, it was obtained about 13-15 nm. As again, there was no solvatochromic behavior observed for **7** and **12** in calculations, as seen experimentally.
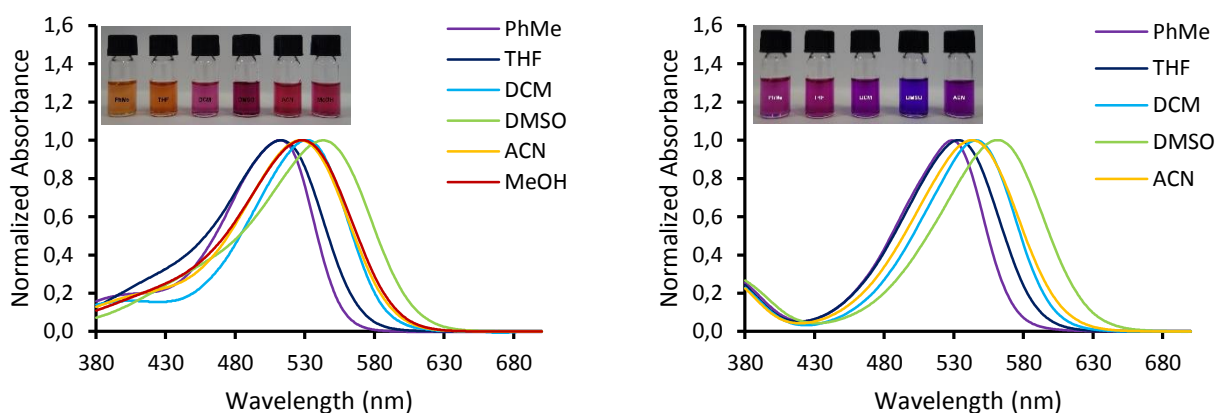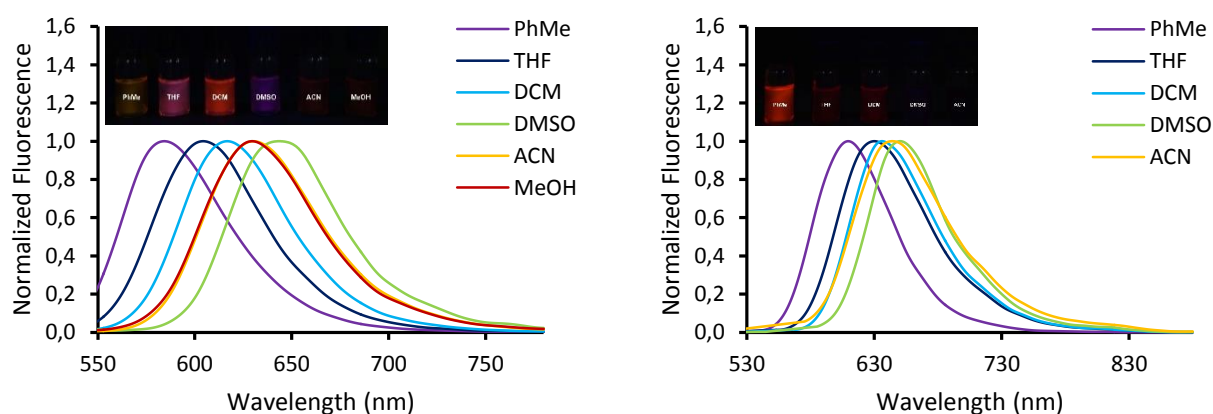
Figure 2. Normalized absorption spectra of compounds **3** (left) and **8** (right) (Inset: Color of compounds **3** and **8** in various solvents with different polarities in ambient light, c=10 µM).

As given in **Table 1**, the calculated absorption maxima correlated with experimental ones for all compounds. In calculations, the main peaks were found to correspond to the H→L transitions from highest occupied molecular orbital (HOMO, H) to lowest unoccupied molecular orbital (LUMO, L) with the highest contributions for **3**, **4**, **5** and **7**. For **6**, the highest contributions were from the transitions H-1→L.

The solvatochromic studies in emission were done in an effort to gain an insight into the photophysical behaviour of these new push-pull dyes bearing free amino and azomethine groups. Therefore, the fluorescence spectra of all dyes **3-7** and **8-12** were recorded in same solvents with various polarities which was used in UV-Vis studies. The results on emission behavior with solvents used are summarized in Table 1 and Table S1 (see SI). The emission properties of all compounds are also essentially regular dependent of the polarity parameter of solvents. However, the largest bathochromic shifts of emission maxima for both serie of compounds were observed

in DMSO. This phenomenon occurs when highly fluorescence polar excited states of push-pull specimens are stabilized by solvents with different polarity [44,45,46,47,48,49,50,51,52]. As examples, the emission spectra of compounds **3** and **8** and the color changes observed upon UV irradiation of both compounds in various solvents are shown in Figure 3. In accordance to both naked eye observation and photographs, only **3** and **8** show solvatochromic effect the most among the series as presented in Figure 3. Solvatochromic phenomenon enhances dramatically under UV light observation where compounds shows considerably different fluorescence color magnitudes with changing polarity except for **12** that is non-fluorescence. Additionally solvent polarity also dictates the emission intensity of all compounds. Polar solvent such as DMSO and methanol yield low fluorescence solution in comparison to less polar solvent like Toluene and THF. This was due to the number of fluorescence inducing aggregates formed by molecules in toluene or THF are greater from those formed in more polar ones [53]. However, the fluorescence property of all compounds was weak in comparison to Fluorescein inside pH 9 that explains low relative quantum yield values, for example 0.0145 for **3** in DCM and 0.116 for **8** in PhMe

Figure 3. Normalized emission spectra of compounds **3** (left) and **8** (right) (Inset: Color of compounds **3** and **8** in various solvents with different polarities in UV irradiation, λ_{ex} = 365 nm, c=1 μM).

Table 1. Photophysical properties of compounds **3-7** in various solvents with different polarity polarity and calculated absorption spectra data.

		experimental						calculated			
	Solvents[a]	λ^{abs}_{max} (nm)	λ^{em}_{max} (nm)	Stokes (nm)	Stokes (cm⁻¹)	Φ_F[b]	ε (mM⁻¹cm⁻¹)	λ^{abs}_{max} (nm)	f	Transitions	w
3	MeOH, (55.4[c])	528	630	102	3074	0.0025	42.625	506	1.1731	H→L	96.2
	ACN (45.6[c])	527	630	103	3125	0.0015	51.729	507	1.1786	H→L	96.2
	DMSO (45.1[c])	543	644	101	2879	0.0086	49.830	511	1.2023	H→L	96.6
	DCM (40.7[c])	531	617	86	2632	0.0145	36.803	506	1.1985	H→L	96.5
	THF (37.4[c])	513	604	91	2961	0.0124	45.871	504	1.1916	H→L	96.4
	PhMe (33.9[c])	512	584	72	2414	0.0074	41.423	494	1.2083	H→L	96.6
4	MeOH	498	606	108	3568	0.0042	55.407	491	1.1403	H→L	89.9
	ACN	495	611	116	3819	0.0039	48.590	492	1.1469	H→L	90.2
	DMSO	510	622	112	3515	0.0069	49.627	495	1.1750	H→L	91.3
	DCM	502	589	87	2954	0.0125	30.143	490	1.1746	H→L	90.9
	THF	486	582	96	3403	0.0083	33.687	488	1.1674	H→L	90.5
	PhMe	488	558	70	2592	0.0042	41.893	478	1.2037	H→L	91.1
5	MeOH	476	609	133	4599	0.0036	39.878	488	1.0314	H-1→L / H→L	15.2 / 84.6
	ACN	473	611	134	4770	0.0032	35.875	489	1.0384	H-1→L / H→L	14.8 / 85.0
	DMSO	486	624	138	4561	0.0067	42.055	492	1.0686	H-1→L / H→L	13.2 / 86.7
	DCM	483	592	109	3828	0.0137	25.315	487	1.0750	H-1→L / H→L	13.4 / 86.4
	THF	457	583	126	4741	0.0066	31.410	485	1.0687	H-1→L / H→L	13.9 / 85.9
	PhMe	467	557	90	3476	0.0046	33.884	476	1.1242	H-1→L / H→L	12.2 / 87.5
6	MeOH	446	600	154	5786	0.0039	40.765	451	0.5104	H-1→L / H→L	62.3 / 37.0
	ACN	442	603	161	6052	0.0034	34.575	451	0.5053	H-1→L / H→L	63.2 / 36.1
	DMSO	463	614	151	5346	0.0046	42.717	453	0.4843	H-1→L / H→L	66.7 / 32.6
	DCM	448	580	132	5099	0.0055	27.791	451	0.4988	H-1→L / H→L	63.2 / 36.1
	THF	439	573	134	5359	0.0062	34.745	450	0.5077	H-1→L / H→L	61.4 / 37.9

|											
	PhMe	440	546	106	4399	0.0041	30.567	446	0.4885	H-1→L H→L	57.8 41.4
7	MeOH	374	-	-	-	-	51.433	419	1.2899	H-1→L	95.0
	ACN	376	-	-	-	-	43.430	419	1.2939	H-1→L	95.0
	DMSO	386	-	-	-	-	40.423	422	1.3123	H-1→L	95.2
	DCM	382	606	224	9705	-	42.125	421	1.3265	H-1→L	94.0
	THF	379	434	55	3357	-	40.418	420	1.3246	H-1→L	93.7
	PhMe	382	577	195	8853	-	53.152	419	1.3788	H-1→L	88.8

[a]Solvents arranged in order of decreasing E_T^{30} values. [b]Fluorescence quantum yield (±10%) determined relative to fluorescein in pH=9 solution (FF = 1.00) as standard. [c]The values for relative polarity are courtesy from Christian Reichardt, *Solvent and Solvent Effect in Organic Chemistry,* Wiley-VCH, 3rd ed., 2003.

Substituent effects

From the investigation, Schiff bases exhibit greater red shift than its styryl counterpart in both absorption and emission spectra, for instance compound **8** reaches its emission maximum at 636 nm whereas compound **3** at 617 nm in DCM. Both styryl and Schiff bases show far greater red shift compared to compared to their previous counterparts [21]. In addition, these results are slightly overshade by triphenylamine-based NLO compounds that were synthetized by our group [19], this explain that triphenylamine is better electron donating group than heterocyclic amines substituent studied in this study. It can be seen from Figure 4 that the absorption maxima of **3-6** and **8-11** depend on the electron-donating substituents and the value increases in the following order: julolidine (**3**,**8**) < pyrolidine (**4**,**9**) < piperidine (**5**,**10**) < morpholine (**6**,**11**). The julolidine substituent containing compounds (**3** and **8**) exhibit the most red shift while 4-morpholinyl substituent show the least. According to our results found showed that while julolidine is the best donating substituent, morpholine is the worst donating. In addition, compound **7** and **12** include 2-pyridyl group and it has electron and proton accepting ability. Therefore, the absorption maxima for **7** and **12** were in the range of

374-386 nm and 377-385 nm, respectively which are lower than others. In addition, the same trends which were obtained from UV-Vis absorption spectra were observed in emission maxima for all compounds.

The observation of intense red shift might be related to significant contribution of ICT (intramolecular electron transfer) for electronic state modification in the excited state of molecules [56]. In this state, all compounds have notably higher dipole moment and lower LUMO energy level compared to their ground state [57]. Increasing electron donating strength of various heterocyclic amines led to the increase of Stokes shift figure and significant red shift between absorption and emission maxima, this is due to varying electronic contributions to the host structure induced by heterocyclic amines constituent [58] (Figure 4).
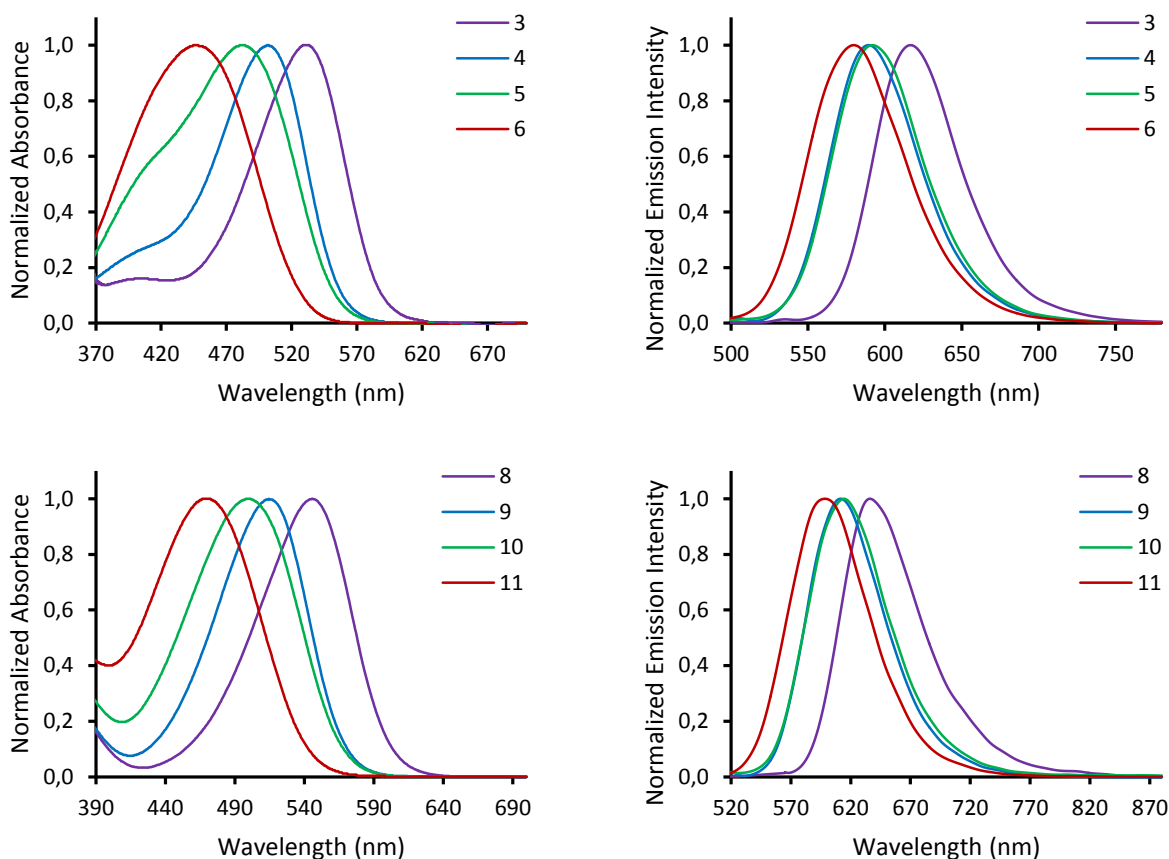
Figure 4. Red shift phenomena with changing of substituent in absorption (left) and emission (right) spectra compound **3-6** (top) and **8-11** (bottom) in DMSO.

Photophysical changes in high pH values

Like others *push-pull* dyes, all synthetized compounds show significant red shift for both emission and absorption maxima with increasing solvent polarity. However, pyridine bearing compounds (**7** and **12**) doesn't show same behavior at all, which was explained by a similar delocalization of the charge in the ground and excited state [60]. This means that these compounds undergo weaker or no ICT phenomenon. Regardless, all compounds that exhibit low intensity fluorescence under excitation at absorption maxima indicate non-radioactive deactivation channel that occurs readily with light source [58].

Neither absorption and emission maxima correlate well with other solvent parameter such as hydrogen-bonding ability, dipole moment, acidity or basicity [54,55]. With this, investigated photophysical changes produce no correlation with solvent polarity as quantified by E_T^{30} which indicates solvent properties other than polarity contribute the molecules stabilization or destabilization in their ground/excited states [59]. Unfortunately, the solubility limitation of all synthetized compounds doesn't allow us to conduct wide range of solvent observation that is required for multiparameter analysis. In conjunction with solvent interaction study hydroxide interaction study was conducted for compound **8-12**. Based on the observations alone compounds **8-12** have the ability to detect hydroxide ion inside DMSO solution. Here they underwent prototopic equilibrium that led to changes of UV-Vis absorption spectra when exposed to basic environment [61]. The interaction between the compound and hydroxide was understood from the bathochromic-shifted maximum of compound **12**, as presented in Figure 5, and the formation of new hypsochromic maximum for other compounds in their UV-Vis absorbance spectrums. In the other hand, all compounds showed an increasing fluorescence intensity with incremental addition of hydroxide ion in the solution. As shown in the Figure 6, compound **12** showed the most fluorescence increase (20,17 folds for 15 OH equiv) marking for its superb sensitivity among the others. The slight increase of emission intensity and the new absorption band is likely due to the phenoxy group is more pronounce electron donor than the phenol group [62]. Furthermore, reversibility test using TFA (Trifluoroacetic acid) shows that all compounds except compound **8** can be brought to initial state hence marks the sensor repeatability usage for every single analysis process.
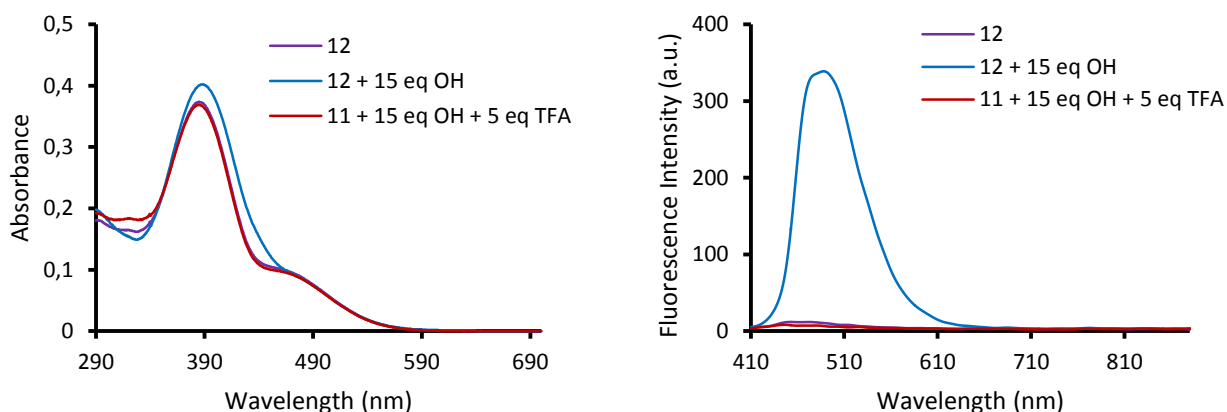
Figure 5. Absorption (left) and emission (right) change of compound **12** upon 15 equiv of TBAOH addition and reverse protonation by 5 equiv of TFA.
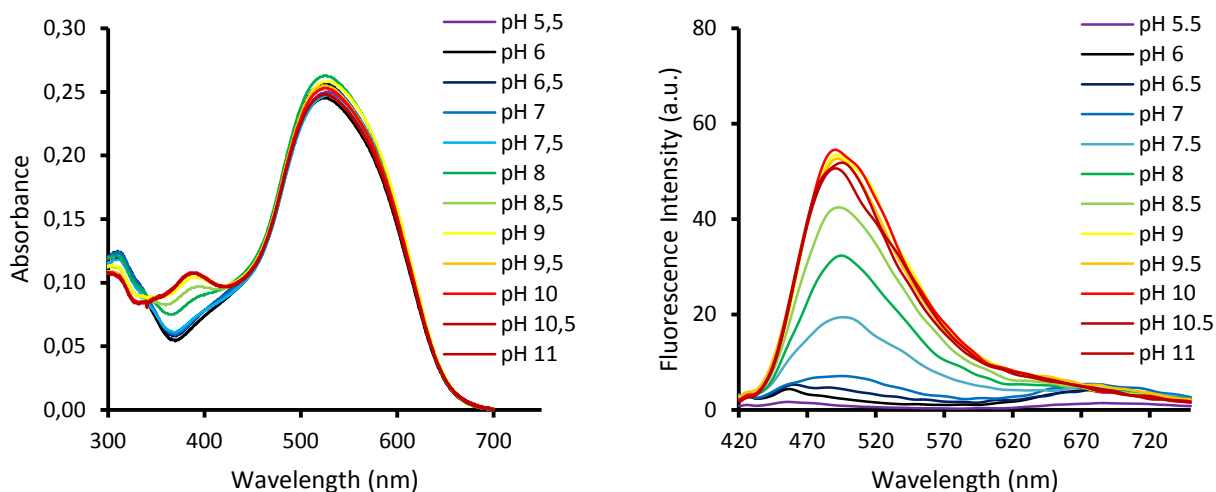

Figure 6. Photographs of compound **12** (left), after the addition of 15 equiv of TBAOH (middle) and reverse protonation (right) by 5 equiv of TFA.

pH sensitive study of 8 in aqueous solution

As how hydroxide ion play critical role in our ecosystem, pH value in water body also does its importance to maintain physiological stability both inside and outside living organism. The pH value remains the most important condition for a natural cycle inside our body in order to run flawlessly, it also judges whether a plant or animal can continue to live in a specific environment. For these reasons, the necessity to develop new kinds of pH sensors has been quite vital in order to control pH condition in the world we lived in. It has been thoroughly studied that optical pH sensor boast for their not having

electrical interference and remarkable sensitivity. Due to their low cost manufacturing and maintenance this class of pH sensor has been met their usages in both clinical and environmental analysis, especially in the form of optrodes [63,64,65]. At the same time, fluorescent pH indicators offer better selectivity and sensitivity than other classes [16]. Aside from that, they provide wide range of measurement techniques such as polarization and energy transfer [14]. Based on this fact we had investigated compound **8** as a future prospect for fluorescent pH sensor.

After examining a good solubility of compound **8** inside fully aqueous solution, hydroxide sensing capability test was performed as an additional study. A number of Britton-Robinson buffer solutions with different pH ranging from 5.5-11 are used both to mimic aqueous environment and to preserve pH stability in solution. As depicted by Figure 5 below, increasing solution of pH has led to a formation of a new band at 393 nm near UV region and weak fluorescence increase at 505 nm. These phenomenon have been accompanied with darkening purple color swifts of the solutions with increasing solution pH, however slight increase in the fluorescence was hardly noticeable under 365 nm UV lamp illumination as shown in the Figure 7.

Figure 6. Absorption (left) and emission (right) change of compound **8** in Britton-Robinson Buffer solutions with different pH.

Figure 7. Photographs of compound **8** in Britton-Robinson Buffer solutions with different pH.

To determine pKa value of organic compound, wide range of methodologies such as solubility measurement [66,67], potentiometry [68,69] and UV-Vis absorption spectroscopy [70,71] can be applied. In our case, determination of pKa of compound **8** has been done using UV-Vis absorption spectroscopy technique. To calculate the figure, we divided newly formed absorption intensity with its own maxima and compared them with corresponding pH values in order to produce a crude sigmoid function. This function was then fitted and rebuilt from scratch using "Curve Fitting"

method and DoseResp approach in order to obtain a clean sigmoid function as shown in the Figure 8 that gave 8.22 ± 0.03 as pKa value of compound **8**.
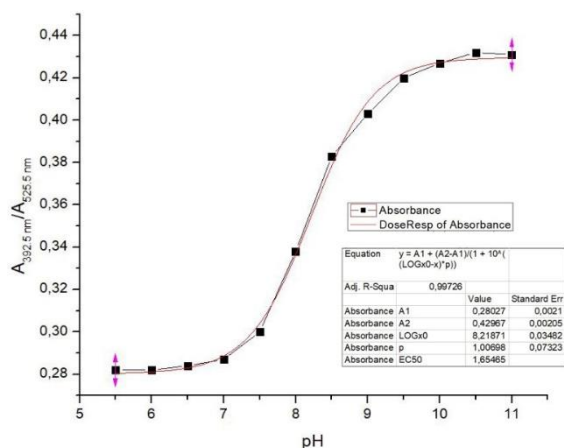
Figure 8. Sigmoid function obtained from compound **8** UV-Vis absorption spectra during pH investigation.

The low absorbance of compound **8** inside Britton-Robinson buffer may be explained by aggregate formation. However, increasing concentration of compound **8** maintains linearity at defined range of calibration graph, thus contradicts aggregation [15].

NLO properties

In order to obtain an insight into the NLO property of the studied compounds, first-order hyperpolarizability (β) and other related measurements such as polarizability (α) and dipole moment (μ) were calculated at B3LYP/6-31+G (d,p) level in gas phase. In general, high NLO response for a typical organic NLO chromophore include donor (D) and acceptor (A) groups linked with a p-conjugation path is characterized by large first order hyperpolarizabity value (β). However, small energy gap between HOMO and

LUMO (E_{gap}) have an important indicator for high NLO responses. Based on the results in Table 2, E_{gap} values obtained on the ground state geometries of compounds change as **3**<**4**~**5**<**6**<**7** for **3-7** and **8**<**9**~**10**<**11**<**12** for **8-12**. The smallest E_{gap} was obtained for **3** and **8** due to the presence of the strongest electron donor group (julolidine), thus, a high NLO response can be expected. As depicted from Table 3 and Table S2 (see SI), the obtained value of the first-order hyperpolarizability (β) was 128.9×10^{-30} esu for **3** and 142.5×10^{-30} esu for **8**. The trends changes as **3**~**5**>**4**>**6**>**7** for **3-7**, **10**>**8**>**9**>**11**>**12** for **8-12**.

Table 2. HOMO and LUMO gap in gas phase for **3-12**.

|	HOMO (eV)	LUMO (eV)	E_{gap} (eV)
3	-5.32	-2.49	2.83
4	-5.51	-2.56	2.95
5	-5.65	-2.68	2.97
6	-5.80	-2.75	3.05
7	-6.15	-3.03	3.12
8	-5.46	-2.73	2.73
9	-5.64	-2.80	2.85
10	-5.64	-2.80	2.83
11	-5.91	-2.97	2.94
12	-6.41	-3.25	3.15

Table 3. For **3-7**, the electric dipole moment (μ), the polarizability (α) and the first hyperpolarizability (β_{tot}) and their components calculated at the B3LYP/6-31+g(d) level in gas phase for all molecules. The components are in a.u.

	3	4	5	6	7
μ_x	3.5805011	3.9333631	2.9683437	-2.5024153	-2.1263813
μ_y	-3.5637062	-3.8420296	-3.4600113	-3.6503204	-4.1533154
μ_z	0.1950602	-0.1593236	0.2224649	0.1989274	0.4316095
μ (D)	**12.85**	**13.98**	**11.60**	**11.26**	**11.91**
α_{xx}	635.2520454	616.7641228	627.7438353	595.7391188	613.5249732
α_{xy}	-39.4558007	-34.754139	-31.1154403	29.4211052	25.2479516
α_{yy}	383.8047364	351.9873818	361.2716177	357.5313289	358.8262369
α_{xz}	8.7091381	8.6393372	13.948762	11.7163478	10.0341376
α_{yz}	0.6802601	0.2560389	1.3076799	0.7790697	-10.140918
α_{zz}	193.1942992	180.0095143	191.6077872	186.8332563	178.7956415
α	**59.9**	**56.7**	**58.3**	**56.3**	**56.9**
$(\times10^{-24})$ esu					
β_{xxx}	-16079.1344	-15567.0831	-16355.8548	14668.67731	6736.315334
β_{xxy}	3439.462528	3226.00696	3022.246246	3004.623196	2148.253767
β_{xyy}	1723.196827	1939.948528	1927.816998	-1948.06104	-2065.91258
β_{yyy}	996.2272236	1187.415397	1384.671036	1389.546732	1690.84885
β_{xxz}	39.8082221	21.2339506	95.5388536	-29.6088314	8.5457476
β_{xyz}	31.0321799	-23.5795344	53.6335744	-90.6200478	-147.983305
β_{yyz}	-51.9668397	-73.8342775	80.2299754	66.9756814	115.5236475
β_{xzz}	73.3267348	69.8310923	182.820974	-142.640148	-32.754675
β_{yzz}	-91.8715934	-101.594229	-112.112264	-109.342561	-97.2160931
β_{zzz}	3.0856498	-16.3804778	140.3169807	-71.7555535	27.8845398
β_{tot}	**128.9**	**122.9**	**128.6**	**114.8**	**51.5**
$(\times10^{-30})$ esu					

Thermal Properties

We conducted thermogravimetric analysis to understand whether the molecule is sufficient for NLO study. Great NLO molecule generally has high thermal dissociation figures for around 250 °C. In NLO study energetic photons tend to emit heat the longer it takes place that's why this thermal condition is crucial for any candidate for NLO

molecules [19,72]. As depicted from Figure 9, mass wise all compounds show non-complete dissociation under inert environment up to 600 °C. All compounds show zero weight loss up from 0 up to 150 °C thus indicates that there is no water or other organic solvent residue on the surface of all compounds. Compounds **8-12** show more lenient weight loss curvatures compared to the Compounds **3-7**'s indicating the Schiff bases are more robust while the styryl compounds tends to dissociate faster when exposed to extreme temperature changes. Based on the results there are no compound that shows more than 1 dissociation steps. All compounds dissociate at the very first step but in an ununiformed manner. Regardless, all compounds show good stability up to around 300 °C while compound **8** as the least thermally stable compound starts to dissociate at around 280 °C. Compared to the literature presented above, these figures indicates that all synthetized compounds are thermally stable hence makes them superb candidates for optoelectronic devices and various NLO applications.
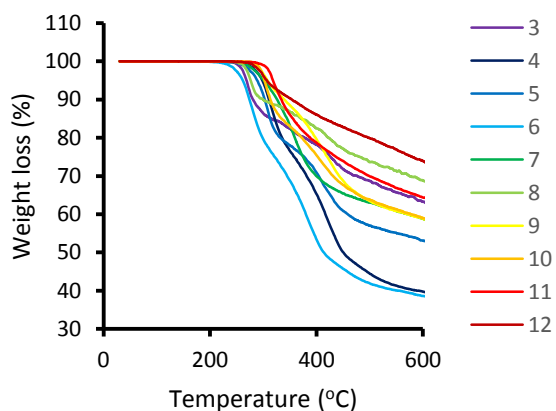
Figure 9. TGA curve of all synthetized compounds

Conclusion

In this study, we have successfully synthetized and characterized a series of new push-pull styryl dyes and their Schiff base associated fluorescent chemosensors that have the ability to detect hydroxide anion in DMSO as well as able to act like pH sensor in fully aqueous environment. In addition, NLO properties of compounds **3-6** and **8-11** were investigated theoretically.

The interaction between the sensor (compound **8-12**) and hydroxide is understood from the bathochromic-shifted maximum of compound **12** and the formation of new hypsochromic maximum for others in their UV-Vis absorbance spectrums. Additionally, all compounds **8-12** showed an increasing fluorescence intensity with incremental addition of hydroxide ion in the solution, compound **12** showed the most fluorescence increase (20,17 folds for 15 OH equiv) marking for its superb sensitivity among others. Furthermore, reversibility test using TFA showed that all Schiff bases except compound **8** can be brought to initial state hence marks their usage repeatability for every single analysis process. The interaction of Schiff base compound and hydroxide in aqueous environment were conducted successfully using compound **8** which has good solubility in water and slight rise of fluorescent is observed with increasing solution of pH.

Thermogravimetric analysis are conducted to understand thermal stability of all synthetized compounds. In general, all compounds both showed a good thermal stability up to around 200 °C and have respectable NLO values from calculation results thus makes them a good candidate for optoelectronic device usages and various NLO applications.

Experimental

Materials, Methods and Instrumentation

All commercially available chemicals were reagent grade and used without further purification. The compounds **1** and **2** which were successfully synthesized from published literatures [42,43]. Thin-layer chromatography (TLC) was used for monitoring the reactions using precoated silica gel 60 F254 plates. Column chromatography was performed on silica gel (60-120 mesh, Merck Chemicals). NMR spectra were measured on Bruker Avance 300 (^{1}H: 300 MHz, ^{13}C: 75 MHz) spectrometers at 20 °C (293 K). Chemical shifts (δ) are given in parts per million (ppm) using the residue solvent peaks as reference relative to TMS. Coupling constants (J) are given in hertz (Hz). Signals are abbreviated as follows: broad. br; singlet. s; doublet. d; doublet-doublet. dd; doublet-triplet dt; triplet. t; multiplet. m. High resolution mass spectra (HRMS) were recorded at Gazi University Faculty of Pharmacy using electron ionization (EI) mass spectrometry (Waters-LCT-Premier-XE-LTOF (TOF-MS) instruments; in m/z (rel. %). The microwave syntheses were carried out in a Milestone Start microwave reaction system. The melting points were measured using Electrothermal IA9200 apparatus. Absorption spectra were recorded on a Shimadzu 1800 spectrophotometer; fluorescence spectra were recorded on a Hitachi F-7000 fluorescence spectrophotometer. The melting points were measured using Electrothermal IA9200 apparatus. Thermal analyses were performed with a Shimadzu DTG-60H system, up to 700 °C (10 °C min^{-1}) under a dynamic nitrogen atmosphere (15 mL min^{-1}).

Photophysical studies

Compounds **3-7** (10 µM for absorption and 1 µM for emission) were studied in six various solvents with different polarity (Toluene, THF, DCM, DMSO, ACN, MeOH), whereas compound **8-12** were studied with the same manner while excluding MeOH due to their low solubilities. All absorption spectra were registered using Shimadzu 1800 spectrophotometer while emission spectra were recorded using Hitachi F-7000 Fluorimeter. All samples were measured inside 1 cm x 1 cm quartz cuvvetes with approximately 2 mL in volume. The deprotonation and reverse protonation studies of compounds **8-12** were conducted inside DMSO. To each DMSO solution 5 equiv of TBAOH were introduced and immediately UV-Vis absorption spectra were taken with the same concentration mentioned above. This titration was repeated until there was no observable change in sample spectra. The titrant used in this titration is 10 mM TBAOH in DMSO. Reverse protonation processes for each compound **8-12** were conducted after TBAOH titration using 10 mM TFA in DMSO, 5 equiv of TFA were introduced to fully deprotonated solutions incrementally until there was no observable change in spectra. All of the procedures above were done at room temperature (25 °C). Emission changes during deprotonation and reverse protonation processes for compound **8-12** were also been registered using fluorimeter in the same manner with the same concentration stated earlier for emission study at room temperature (25 °C). All photographs were taken using SONY RX100 pocket camera with ISO values of 200 and variable aperture at "Program Auto" mode.

pKa determination for Compound 8

Solubility of compound **8** in deionized water were conducted by studying its calibration graph at 505 nm. The calibration graph was obtained using UV-Vis absorption spectrophotometry by the following procedure, 5 µM of **8** solution were prepared and

immediately its absorbance at 505 nm were registered, into the same solution 10 µL from 1 mM compound **8**'s stock solution were added incrementally followed by recording its absorbance value after each addition. From the results absorbance vs Concentration graph was drawn in order to obtain the calibration graph and its linearity were investigated by calculating R^2 value in Microsoft Excel.

The spectra of compound **8** were recorded using Shimadzu 1800 spectrophotometer in Britton-Robinson buffer solutions [79] with pH values ranging from 5.5 to 11 at room temperature (25 °C). Determination of compound **8** pKa has been done by dividing new band wavelength intensity with its own maxima and compared them with corresponding pH values which led to a crude sigmoid function. Obtained function was then fitted and rebuilt from scratch using "Curve Fitting" method and DoseResp approach in order to obtain a clean sigmoid function.

Computational methods

The geometry of all compounds in their ground states have been calculated by Density Functional Theory at B3LYP/6-31+G(d,p) level in gas phase [80,81]. This method were also applied to study non-linear optic (NLO) property of each compounds on their ground states. Theoretical absorption spectra in different solvents were calculated with time dependent DFT (TD-DFT) method at the same level. For calculations in solvents, Polarizable Continuum Model (PCM) was used [82,83]. All the calculations were done using Gaussian 09 program [84].

General synthesis procedure of compound 3-7

A mixture of 3 mmol 2-(1-(4-aminophenyl)ethylidene)malononitrile (**1**) and its equivalent mol amount of appropriate benzaldehyde was solved in 20 mL ethanol and

refluxed for 2 hours straight. The colored solid was then filtered off and recrystallized by ethanol in order to obtain a pure compound.

Compound **3** (*(E)-2-(1-(4-aminophenyl)-3-(2,3,6,7-tetrahydro-1H,5H-pyrido[3,2,1-ij]quinolin-9-yl)allylidene)malononitrile*)

(Yield: 64 %, mp: 236-238 °C) FT-IR (cm^{-1}): 3441, 3349, 3224, 2920, 2836, 2202, 1633, 1603, 1568, 1519, 1467. ^{1}H NMR (300 MHz, DMSO-d_6) δ 7.15 (d, J = 8.5 Hz, 2H), 7.05 (m, 3H), 6.85 (d, J = 14.9 Hz, 1H), 6.65 (m, 2H), 5.96 (s, 2H), 3.27 (t, J = 5.8 Hz, 4H), 2.66 (t, J = 6.2 Hz, 4H), 1.84 (p, J = 6.2 Hz, 4H). ^{13}C NMR (75 MHz, DMSO-d_6) δ 171.7, 153.5, 153.4, 149.1, 132.3, 131.2, 124.8, 120.6, 120.0, 116.5, 115.7, 114.5, 113.6, 72.4, 66.3, 47.3, 44.6. HR-MS (*m/z*), (M-H)$^{+\cdot}$: C$_{24}$H$_{22}$N$_4$ calculated: 367.1923; found: 367.1918.

Compound **4** (*(E)-2-(1-(4-aminophenyl)-3-(4-(pyrrolidin-1-yl)phenyl)allylidene)malononitrile*)

(Yield: 58 %, mp: 199-201 °C) FT-IR (cm^{-1}): 3435, 3343, 3227, 2971, 2860, 2205, 1609, 1569, 1521, 1471. ^{1}H NMR (300 MHz, DMSO-d_6) δ 7.52 (d, J = 8.5 Hz, 2H), 7.18 (m, 3H), 6.98 (d, J = 15.1 Hz, 1H), 6.67 (d, J = 8.3 Hz, 2H), 6.60 (d, J = 8.6 Hz, 2H), 6.01 (s, 2H), 3.34 (s, 4H), 1.98 (d, J = 6.6 Hz, 4H). ^{13}C NMR (75 MHz, DMSO-d_6) δ 171.7, 153.0, 150.5, 150.2, 132.1, 131.8, 122.0, 120.2, 118.2, 116.8, 116.0, 113.6, 112.6, 70.7, 47.9, 25.4. HR-MS (*m/z*), (M-H)$^{+\cdot}$: C$_{22}$H$_{20}$N$_4$ calculated: 341.1766; found: 341.1777.

Compound **5** (*(E)-2-(1-(4-aminophenyl)-3-(4-(piperidin-1-yl)phenyl)allylidene)malononitrile*)

(Yield: 75 %, mp: 193-194 °C) FT-IR (cm^{-1}): 3460, 3366, 3222, 2933, 2918, 2814, 2204, 1628, 1573, 1545, 1471. ^{1}H NMR (300 MHz, DMSO-d_6) δ 7.50 (m, 2H), 7.20 (m, 3H),

6.96 (m, 3H), 6.66 (m, 2H), 6.05 (s, 2H), 3.39 (s, 4H), 1.57 (s, 6H). ^{13}C NMR (75 MHz, DMSO-d_6) δ 171.7, 153.5, 153.4, 149.1, 132.3, 131.2, 124.8, 120.6, 120.0, 116.5, 115.7, 114.5, 113.6, 72.4, 66.3, 47.3, 44.6. HR-MS (*m/z*), (M-H)$^{+\cdot}$: C$_{23}$H$_{22}$N$_4$ calculated: 355.1923; found: 355.1924.

Compound **6** (*(E)-2-(1-(4-aminophenyl)-3-(4-(morpholin-1-yl)phenyl)allylidene)malononitrile*)

(Yield: 70 %, mp: 168-169 °C) FT-IR (cm^{-1}): 3467, 3372, 3215, 3033, 2955, 2828, 2210, 1629, 1581, 1512, 1478. ^{1}H NMR (300 MHz, DMSO-d_6) δ 7.57 (d, *J* = 8.6 Hz, 2H), 7.24 (m, 3H), 6.99 (m, 3H), 6.67 (d, *J* = 8.4 Hz, 2H), 6.09 (s, 2H), 3.72 (t, *J* = 4.8 Hz, 4H), 3.29 (d, *J* = 4.9 Hz, 4H). ^{13}C NMR (75 MHz, DMSO-d_6) δ 171.7, 153.5, 153.4, 149.1, 132.3, 131.2, 124.8, 120.6, 120.0, 116.5, 115.7, 114.5, 113.6, 72.4, 66.3, 47.3. HR-MS (*m/z*) , (M-H)$^{+\cdot}$: C$_{22}$H$_{20}$N$_4$O calculated: 357.1715; found: 357.1716.

Compound **7** (*(E)-2-(1-(4-aminophenyl)-3-(4-(pyridin-1-yl)phenyl)allylidene)malononitrile*)

(Yield: 64 %, mp: 214-215 °C) FT-IR (cm^{-1}): 3488, 3384, 3221, 3036, 2211, 1597, 1512, 1476, 1463. ^{1}H NMR (300 MHz, DMSO-d_6) δ 8.70 (m, 1H), 8.19 (d, *J* = 8.3 Hz, 2H), 8.05 (m, 1H), 7.91 (td, *J* = 1.8, 7.7 Hz, 1H), 7.84 (d, *J* = 8.4 Hz, 2H), 7.51 (d, *J* = 15.6 Hz, 1H), 7.37 (m, 3H), 7.17 (d, *J* = 15.6 Hz, 1H), 6.70 (m, 2H), 6.25 (s, 2H). ^{13}C NMR (75 MHz, DMSO-d_6) δ 170.9, 155.3, 154.0, 150.2, 147.4, 141.2, 137.8, 135.6, 132.8, 129.6, 127.6, 125.8, 123.7, 121.1, 119.6, 116.1, 115.2, 113.7, 75.0. HR-MS (*m/z*), (M-H)$^{+\cdot}$: C$_{23}$H$_{16}$N$_4$ calculated: 349.1453; found: 349.1458.

General synthesis procedure of compound 8-12

A mixture of 1 mmol of appropriate styryl compound (3-7) and 8 mmol of salicyaldehyde was solved in 10 mL ethanol and refluxed for half an hour. The colored solid was then filtered off and recrystallized by ethanol in order to obtain a pure compound.

Compound **8** (*2-((E)-1-(4-(((E)-2-hydroxybenzylidene)amino)phenyl)-3-(2,3,6,7-tetrahydro-1H,5H-pyrido[3,2,1-ij]quinolin-9-yl)allylidene)malononitrile*)

(Yield: 94 %, mp: 202-203 °C) FT-IR (cm^{-1}): 3479 (broad), 3062, 2943, 2835, 2208, 1614, 1560, 1510, 1469. ^{1}H NMR (300 MHz, DMSO-d_6) δ 12.80 (s, 1H), 9.05 (s, 1H), 7.70 (d, J = 7.6 Hz, 1H), 7.52 (m, 5H), 7.09 (m, 5H), 6.75 (d, J = 14.9 Hz, 1H), 2.65 (t, J = 6.2 Hz, 4H), 1.83 (p, J = 5.9 Hz, 4H). ^{13}C NMR (75 MHz, DMSO-d_6) δ 171.0, 165.2, 160.8, 153.6, 150.8, 150.3, 136.9, 134.2, 133.1, 132.3, 132.1, 131.0, 123.5, 123.0, 122.3, 119.8, 118.9, 117.2, 115.4, 114.6, 114.5, 114.4, 114.3, 95.7, 75.8, 48.1, 25.4, 24.4. HR-MS (*m/z*), (M-H)$^{+\cdot}$: C$_{31}$H$_{26}$N$_4$O calculated: 471.2185; found: 471.2162.

Compound **9** (*2-((E)-1-(4-(((E)-2-hydroxybenzylidene)amino)phenyl)-3-(4-(pyrrolidin-1-yl)phenyl)allylidene)malononitrile*)

(Yield: 96 %, mp: 234-235 °C) FT-IR (cm^{-1}): 3394 (broad), 3035, 2972, 2865, 2206, 1616, 1588, 1523, 1475. ^{1}H NMR (300 MHz, DMSO-d_6) δ 12.81 (s, 1H), 9.06 (s, 1H), 7.71 (d, J = 7.7 Hz, 1H), 7.53 (m, 7H), 7.26 (d, J = 15.0 Hz, 1H), 7.01 (t, J = 8.0 Hz, 2H), 6.89 (d, J = 15.1 Hz, 1H), 6.60 (d, J = 8.5 Hz, 2H), 3.35 (s, 4H), 1.96 (s, 4H). ^{13}C NMR (75 MHz, DMSO-d_6) δ 192.2, 165.2, 161.2, 160.8, 153.0, 150.5, 150.2, 136.9, 133.1, 132.1, 131.8, 130.9, 129.7, 122.3, 122.0, 120.3, 119.9, 118.2, 117.7, 117.2, 116.8, 113.6, 112.8, 112.6, 70.7, 47.9, 47.8, 25.3. HR-MS (*m/z*), (M-H)$^{+\cdot}$: C$_{29}$H$_{24}$N$_4$O calculated: 453.1715; found: 453.1715.

Compound **10** (*2-((E)-1-(4-(((E)-2-hydroxybenzylidene)amino)phenyl)-3-(4-(piperidin-1-yl)phenyl)allylidene)malononitrile*)

(Yield: 95 %, mp: 212-213 °C) FT-IR (cm⁻¹): 3319 (broad), 3043, 2925, 2846, 2212, 1620, 1574, 1515, 1464. ^{1}H NMR (300 MHz, DMSO-d_6) δ 12.80 (s, 1H), 9.06 (d, J = 4.7 Hz, 1H), 7.71 (d, J = 7.5 Hz, 1H), 7.54 (m, 8H), 7.30 (dd, J = 4.0, 15.4 Hz, 1H), 6.95 (m, 4H), 3.41 (t, J = 5.0 Hz, 4H), 1.57 (s, 6H). ^{13}C NMR (75 MHz, DMSO-d_6) δ 171.0, 165.2, 160.8, 153.6, 150.8, 150.3, 136.9, 134.2, 133.1, 132.3, 132.1, 131.0, 123.5, 123.0, 122.3, 119.8, 118.9, 117.2, 115.4, 114.6, 114.5, 114.4, 114.3, 95.7, 75.8, 48.1, 25.4, 24.4. HR-MS (m/z), (M-H)$^{+\cdot}$: C$_{30}$H$_{26}$N$_4$O calculated: 459,2185; found: 459.2175.

Compound **11** (*2-((E)-1-(4-(((E)-2-hydroxybenzylidene)amino)phenyl)-3-(4-(morpholin-1-yl)phenyl)allylidene)malononitrile*)

(Yield: 93 %, mp: 187-188 °C) FT-IR (cm⁻¹): 3404 (broad), 3094, 2969, 2848, 2217, 2207, 1615, 1586, 1516, 1489. ^{1}H NMR (300 MHz, DMSO-d_6) δ 12.79 (s, 1H), 9.07 (s, 1H), 7.71 (dd, J = 1.7, 7.9 Hz, 1H), 7.59 (q, J = 3.2, 4.2 Hz, 6H), 7.46 (td, J = 1.7, 7.8 Hz, 1H), 7.36 (d, J = 15.3 Hz, 1H), 6.97 (m, 5H), 3.71 (t, J = 4.8 Hz, 4H), 3.31 (t, 4H). ^{13}C NMR (75 MHz, DMSO-d_6) δ 192.2, 171.1, 165.2, 160.8, 153.8, 150.9, 150.1, 136.9, 134.2, 133.1, 132.3, 132.1, 131.8, 131.2, 131.0, 129.6, 124.4, 122.3, 119.9, 119.8, 117.7, 117.2, 114.4, 113.6, 77.1, 66.3, 47.3, 47.1. HR-MS (m/z), (M-H)$^{+\cdot}$: C$_{29}$H$_{24}$N$_4$O$_2$ calculated: 461.1978; found: 461.1961.

Compound **12** (*2-((E)-1-(4-(((E)-2-hydroxybenzylidene)amino)phenyl)-3-(4-(pyridin-1-yl)phenyl)allylidene)malononitrile*)

(Yield: 59 %, mp: 205-206 °C) FT-IR (cm⁻¹): 3600-3000 (broad), 3048, 2217, 1620, 1594, 1568, 1488, 1453. ^{1}H NMR (300 MHz, DMSO-d_6) δ 12.77 (s, 1H), 9.08 (s, 1H), 8.70 (m, 1H), 8.21 (d, J = 8.2 Hz, 2H), 8.06 (d, J = 8.0 Hz, 1H), 7.90 (m, 3H), 7.73 (m, 1H), 7.66 (m, 5H), 7.48 (dd, J = 1.7, 7.6 Hz, 1H), 7.41 (m, 1H), 7.12 (s, 1H), 7.03 (m,

3H). ^{13}C NMR (75 MHz, DMSO-d_6) δ 192.2, 191.6, 165.3, 160.8, 155.2, 154.0, 150.2, 149.6, 137.9, 136.9, 133.1, 132.8, 131.2, 130.7, 130.0, 129.6, 129.4, 129.1, 127.6, 127.6, 127.0, 122.5, 119.9, 119.8, 119.4, 117.7, 117.2, 113.7, 113.1, 95.7. HR-MS (*m/z*), (M-H)$^{+\cdot}$: $C_{30}H_{20}N_4O$ calculated: 453.1715; found: 453.1715.

Supporting Information

Supporting information text

Supporting Information File 1:

File Name: BJOC_SI_AIO

File Format: .docx

Title: Additional experimental, photophysical and calculated data

Acknowledgements

References

1. Valeur, B.; Berberan-Santos Mário Nuno. *Molecular fluorescence: principles and applications*, **2013,** Weinheim: Wiley-VCH.
2. Gore, M. G. *Spectrophotometry and spectrofluorimetry: a practical approach*, **2000,** Oxford: Oxford University Press.

3. Braslavsky, S. E. *Glossary of terms used in photochemistry: (Iupac recommendations 2006)*, **2007,** Research Triangle Park, NC: Pure and Applied Chemistry.

4. Williams, D. J. *Angew. Chem. Int. Ed.*, **1984,** *23*(9), 690-703.

5. Boyd, R. W. *Nonlinear optics*, **2003,** Elsevier.

6. Marder, S. R.; Beratan, D. N.; Cheng, L. T. *Science*, **1991,** *252*(5002), 103-106.

7. Eaton, D. F. *Science*, **1991,** *253*(5017), 281-287.

8. Zheng, X.; McLaughlin, C. V.; Cunningham, P.; Hayden, L. M. *J. Nanoelectron. Optoe.,* **2007,** *2*(1), 58-76.

9. Dalton, L. R.; Sullivan, P. A.; Bale, D. H. *Chem. Rev.,* **2009,** *110*(1), 25-55.

10. Benassi, E.; Egidi, F.; Barone, V. *J. Phys. Chem. B.*, **2015,** *119*(7), 3155-3173.

11. Cole, J. M. *Philos. Trans. Royal. Soc. A.*, **2003,** *361*(1813), 2751-2770.

12. (a) Czarnik, A. W. *Chem. Biol.*, **1995,** *2*(7), 423-428. (b) Yan, N. D. *Can. J. Fish. Aquat. Sci.*, **1983,** *40*(5), 621-626. (c) GERLOFF-ELIAS, A. N. T. J. E.; Spijkerman, E.; PRÖSCHOLD, T. *Plant. Cell. Environ.*, **2005,** *28*(10), 1218-1229. (d) Lee, K. H.; Lee, H. Y.; Lee, D. H.; Hong, J. I. *Tetrahedron Lett.*, **2001,** *42*(32), 5447-5449.

13. Fayed, T.; EL-Morsi, M.; EL-Nahass, M. *J. Chem. Sci.* **2013,** *125*, 883-894.

14. Wencel, D.; Abel, T.; McDonagh, C. *Anal. Chem.* **2013,** 86(1), 15-29.

15. Arslan, Ö.; Aydıner, B.; Yalçın, E.; Babür, B.; Seferoğlu, N.; Seferoğlu, Z. *J. Mol. Struct.*, **2017**, *1149*, 499-509.

16. Fang, M.; Adhikari, R.; Bi, J.; Mazi, W.; Dorh, N.; Wang, J.; Tiwari, A. *J. Mater. Chem. B*, **2017**, *5*(48), 9579-9590.

17. Jarrahpour, A.; Khalili, D.; De Clercq, E.; Salmi, C.; Brunel, J. *Molecules*, **2007,** *12*(8), 1720-1730.

18. Chow, M. J.; Licona, C.; Yuan Qiang Wong, D.; Pastorin, G.; Gaiddon, C.; Ang, W. H. *J. Med. Chem.*, **2014,** *57*(14), 6043-6059.

19. Çatal, E.; Keleş, E.; Seferoğlu, N.; Achelle, S.; Barsella, A.; Le Guen, F. R.; Seferoğlu, Z. *New J. Chem.*, **2018,** *42*(18), 15052-15060.

20. Aksungur, T.; Aydıner, B.; Seferoğlu, N.; Özkütük, M.; Arslan, L.; Reis, Y.; Seferoğlu, Z. *J. Mol. Struct.*, **2017,** *1147*, 364-379.

21. Yalçın, E.; Achelle, S.; Bayrak, Y.; Seferoğlu, N.; Barsella, A.; Seferoğlu, Z. *Tetrahedron Lett.,* **2015,** *56*(20), 2586-2589.

22. Bardasov, I. N.; Alekseeva, A. U.; Chunikhin, S. S.; Shishlikova, M. A.; Ershov, O. V. *Tetrahedron Lett.*, **2019,** *60*(17), 1170-1173.

23. Shimizu, S.; Watanabe, N.; Kataoka, T.; Shoji, T.; Abe, N.; Morishita, S.; Ichimura, H. *Ullmanns Encyclopedia of Industrial Chemistry*, **2000,** Willey

24. Bruttel, P.; Schlink, R. *Metrohm monograph,* **2003,** *8*(026), 50003.

25. Su, J. Y.; Lo, C. Y.; Tsai, C. H.; Chen, C. H.; Chou, S. H.; Liu, S. H.; Wong, K. T. *Org. Lett.*, **2014,** *16*(12), 3176-3179.

26. Shinar, J.; Shinar, R. *J. Phys. D. Appl. Phys.*, **2008,** *41*(13), 133001.

27. Browning, C. H.; Cohen, J. B.; Ellingworth, S.; Gulbransen, R. *Brit. Med. J.,* **1923,** *2*(3269), 326.

28. Eller, K.; Henkes, E.; Rossbacher, R.; Höke, H. *Ullmann's Encyclopedia of Industrial Chemistry*, **2000**. Willey.

29. Vitaku, E.; Smith, D. T.; Njardarson, J. T. *J. Med. Chem.,* **2014,** *57*(24), 10257-10274.

30. Higashio, Y.; Shoji, T. *Appl. Catal. A. Gen.,* **2004,** *260(2)*, 251-259.

31. Gonzalez, J. M.; Greenway, G. M.; McCreedy, T.; Qijun, S. *Analyst,* **2000,** *125*(4), 765-769.

32. Russell, P. E. *J. Agric. Sci.,* **2005,** *143*(1), 11-25.

33. Haidekker, M. A.; Brady, T. P.; Lichlyter, D.; Theodorakis, E. A. *Bioorg. Chem.,* **2005,** *33*(6), 415-425.

34. Wu, J.; Wang, W.; Wang, N.; He, J.; Deng, G.; Li, Z.; Chen, K. *Phys. Chem. Chem. Phys.,* **2018,** *20*(36), 23606-23615.

35. Zhang, H.; Huo, F.; Liu, F.; Chen, Z.; Liu, J.; Bo, S.; Qiu, L. *RSC Adv.,* **2016,** *6*(102), 99743-99751.

36. Hijji, Y. M.; Barare, B.; Kennedy, A. P.; Butcher, R. *Sens. Actuators. B. Chem.*, **2009,** *136*(2), 297-302.

37. Udhayakumari, D.; Velmathi, S.; Boobalan, M. S. *J. Fluor. Chem.*, **2015,** *175*, 180-184.

38. Barare, B.; Yıldız, M.; Ünver, H.; Aslan, K. *Tetrahedron Lett.*, **2016,** *57*(5), 537-542.

39. Zhang, X.; Chen, S.; Jin, S.; Zhang, Y.; Chen, X.; Zhang, Z.; Shu, Q. *Sens. Actuators. B. Chem.*, **2017,** *242*, 994-998.

40. Chemchem, M.; Yahaya, I.; Aydıner, B.; Seferoğlu, N.; Doluca, O.; Merabet, N.; Seferoğlu, Z. *Tetrahedron,* **2018,** *74*(48), 6897-6906.

41. Marder, S. R. *J. Mater. Chem.*, **2009,** *19*(40), 7392-7393.

42. Zitzler-Kunkel, A.; Lenze, M. R.; Kronenberg, N. M.; Krause, A. M.; Stolte, M.; Meerholz, K.; Würthner, F. *Chem. Mater.*, **2014,** *26*(16), 4856-4866.

43. Breitung, E. M.; Shu, C. F.; McMahon, R. J. *J. Am. Chem. Soc.*, **2000,** *122*(6), 1154-1160.

44. Tydlita´t, J.; Achelle, S.; Rodrı´guez-Lo´pez, J.; Pytela, O.; Miky´sek, T.; Cabon, N.; Robin-le-Guen, F.; Miklı´k, D.; Ru˚zˇicˇkova´, Z.; Buresˇ, F. *Dyes Pigm.*, **2017,** *146*, 467.

45. Cvejn, D.; Achelle, S.; Pytela, O.; Malval, J.-P.; Spangenberg, A.; Cabon, N.; Buresˇ, F.; Robin-le Guen, F. *Dyes Pigm.*, **2016,** *124*, 101.

46. Le Droumaguet, C.; Soudron, A.; Genin, E.; Mongin, O.; Blanchard-Desce, M. *Chem. – Asian J.*, **2013,** *8*, 2984.

47. Fonseca, R. D.; Vivas, M. G.; Silva, D. L.; Eucat, G.; Bretonnie`re, Y.; Andraud, C.; De Boni, L.; Mendonça, C. R. *J. Phys. Chem. C*, **2018,** *122*, 1770

48. Erande, Y.; Kothavale, S.; Sreenath, M. C.; Chitrambalam, S.; Joe, I. H.; Sekar, N. *Dyes Pigm.*, **2018,** *148*, 474.

49. Hoffert, K.; Durand, R. J.; Gauthier, S.; Robin-le-Guen, F.; Achelle, S. *Eur. J. Org. Chem.*, **2017,** 523.

50. Denneval, C.; Achelle, S.; Baudequin, C.; Robin-le-Guen, F. *Dyes Pigm.*, **2014,** *110*, 49.

51. Katan, C.; Terenziani, F.; Mongin, O.; Wertz, M. H. W.; Porre`s, L.; Pons, T.; Mertz, J.; Tretiak, S.; Blanchard-Desce, M. *J. Phys. Chem. A*, **2005,** *109*, 3024.

52. Lartia, R.; Allain, C.; Bordeau, G.; Schmidt, F.; Fiorini-Debuisschert, C.; Charra, F.; Teulade-Fichou, M.-P. *J. Org. Chem.*, **2008,** *73*, 1732.

53. Gadde, S.; Batchelor; E. K., Weiss; J. P.; Ling, Y.; Kaifer, A. *J. Am. Chem. Soc.*, **2008,** *130*, 17114.

54. Lakowicz, J. R. *Principles of Fluorescence Spectroscopy*; Springer, 2006. doi:10.1007/978-0-387-46312-4

55. Valeur, B.; Berberan-Santos, M. N. *Molecular fluorescence. Principles and applications*, 2nd ed.; Wiley-VCH: Weinheim, 2012. doi:10.1002/9783527650002

56. Bergen, A.; Granzhan, A.; Ihmels, H. *Photochem. Photobiol. Sci.* **2008**, *7*(4), 405-407.

57. Suppan, P.; Ghoneim, N. *Solvatochromism;* RSC: Cambridge, 1997.

58. Coelho, F. L.; de Ávila Braga, C.; Zanotto, G. M.; Gil, E. S.; Campo, L. F.; Gonçalves, P. F. B.; da Silveira Santos, F. *Sens. Actuators B: Chem.* **2018**, 259, 514-525.

59. Reichardt, C. *Chem. Rev.*, **1994,** *94*(8), 2319-2358.

60. Hu, J.; Xia, B.; Bao, D.; Ferreira, A.; Wan, J.; Jones, G., II; Vullev, V. I. *J. Phys. Chem. A* **2009**, 113, 3096–3107. doi:10.1021/jp810909v

61. Schäfer, K.; Ihmels, H.; Bohne, C.; Valente, K. P.; Granzhan, A. *J. Org. Chem.* **2016,** 81(22), 10942-10954.

62. Hansch, C.; Leo, A.; Taft, R. W. *Chem. Rev.* **1991**, 91, 165.

63. Lindner, E.; Zwickl, T.; Bakker, E.; Lan, B.T.T.; Tóth, K.; Pretsch, E. *Anal. Chem.* **1998**, 70, 1176–1181.

64. Hisamoto, H.; Tsubuku, M.; Enomoto, T.; Watanabe, K.; Kawaguchi, H.; Koike, Y.; Suzuki, K. *Anal. Chem.* **1996**, 68, 3871–3878.

65. Safavi, A.; Bagheri, M. *Sens. Actuators B: Chem.* **2003,** 90, 143–150.

66. Grbic, S.; Parojcic, J.; Malenovic, A.; Djuric, Z.; Maksimovic, M. *J. Chem. Eng. Data* **2010**, 55, 1368–1371.

67. Antonilli, M.; Bottari, E.; Festa, M.R.; Gentile, L. *J. Chem. Eng. Data*, **2010,** 55, 3373–3378.

68. Jabbari, M.; Gharib, F. *J. Solut. Chem.* **2011**, 40, 561–574.

69. Meloun, M.; Ferenˇcíková, Z.; Vrána, A. *J. Chem. Thermodyn.* **2011**, 43, 930–937.

70. Benvidi, A.; Heidari, F.; Tabaraki, R.; Mazloum-Ardakani, M. *Acta A Mol. Biomol. Spectrosc.* **2011**, 78, 1380–1385.

71. Sanli, S.; Sanli, N.; Alsancak, G. *ActaChim. Slov.* **2010**, 57, 980–987.

72. Britto Dhas, S. M.; Natarajan, S. *Cryst. Res. Technol.: J. Exp. Ind. Crystallogr.* **2007,** 42(5), 471-476.

73. Lanke, S. K.; Sekar, N. *J. Fluoresc.,* **2016,** *26*(3), 949-962.

74. Achelle, S.; Malval, J.-P.; Aloise, S.; Barsella, A.; Spangenberg, A.; Mager, L.; Akdas-Kilig, H.; Fillaut, J.-L.; Caro, B.; Robin-le Guen, F. *Chem. Phys. Chem.*, **2013,** *14*, 2725–2736.

75. Klikar, M.; Bureš, F.; Pytela, O.; Mikysek, T.; Padeˇlkova, Z.; Barsella, A.; Dorkenoo, K.; Achelle, S. *New J. Chem.,* **2013,** *37,* 4230–4240.

76. Achelle, S.; Kahlal, S.; Barsella, A.; Saillard, J.-Y.; Che, X.; Vallet, J.; Bureš, F.; Caro, B.; Robinle Guen, F. *Dyes Pigm.*, **2015,** *113*, 562–570.

77. Achelle, S.; Barsella, A.; Baudequin, C.; Caro, B.; Robin-le Guen F. *J. Org. Chem.* **2012,** *77,* 4087–4096.

78. Gauthier, S.; Vologdin, N.; Achelle, S.; Barsella, A.; Caro, B.; Robin-le Guen, F. *Tetrahedron*, **2013,** *69*, 8392–8399.

79. Britton, H. T. S.; Robinson, R.A. *J. Chem. Soc.*, **1931**, 1456–1462.

80. Lee, C.T.; Yang, W.T.; Parr, R.G. Phys Rev B **1988**, 37, 785-789.

81. Becke, A.D. J. Chem. Phys. **1993**, 98(7), 5648-5652.

82. Cossi, M.; Barone, V. J. Chem. Phys. **2001**, 115, 4708-4717.

83. Bauernschmitt, R.; Ahlrichs, R. Chem.Phys. Lett. **1996**, 256, 454-464.

84. Frisch, M. J.; Trucks, G. W.; Schlegel, H. B.; Scuseria, G. E.; Robb, M. A. et. al Gaussian 09, Revision C.01, Gaussian, Inc., Wallingford CT, 2010.